*Journal of The Electrochemical Society,* **148** (1) C21-C27 (2001)
S0013-4651/2001/148(1)/C21/7/$7.00 © The Electrochemical Society, Inc.

# Interlayer Mediated Epitaxy of Cobalt Silicide on Silicon (100) from Low Temperature Chemical Vapor Deposition of Cobalt

## Formation Mechanisms and Associated Properties

**Ana R. Londergan,[a,d] Guillermo Nuesca,[a] Cindy Goldberg,[a,e] Gregory Peterson,[a] Alain E. Kaloyeros,[a,Z] Barry Arkles,[b] and John J. Sullivan[c,*]**

[a]*New York State Center for Advanced Thin Film Technology and Department of Physics, The University at Albany-State University of New York, Albany, New York 1222, USA*
[b]*Gelest Incorporated, Tullytown, Pennsylvania 19007, USA*
[c]*MKS Instruments, Andover, Massachusetts 01810, USA*

This paper reports the development of a methodology for the growth of epitaxial $CoSi_2$ that uses Co films deposited by low temperature (390°C) chemical vapor deposition (CVD) from cobalt tricarbonyl nitrosyl [$Co(CO)_3NO$] as source precursor. This CVD process exploits the reaction kinetics associated with the adsorption and decomposition of $CoCO)_3NO$ on Si surfaces to ensure the *in situ,* sequential growth of an ultrathin interfacial oxide layer followed by a Co thin film in a single deposition step. It is demonstrated that this interlayer, consisting of a Si–O or a Co-Si-O phase, inhibits silicidation for uncapped CVD Co regardless of annealing times and temperatures. Instead, Co agglomeration is observed, with the degree of agglomeration being proportional to the annealing temperature. The agglomeration is due to a reduction in the overall energy of the system through decrease of the Co/substrate interfacial area. Alternatively, for Ti/TiN capped CVD Co samples, the interfacial layer appears to play a role similar to that observed for similar layers in interlayer mediated epitaxy (IME). This assessment is supported by the observation of epitaxial $CoSi_2$ for capped CVD Co samples after a single-step anneal at 725°C for 30 s. In contrast, Ti/TiN capped PVD Co samples annealed under identical processing conditions exhibited a polycrystalline $CoSi_2$ phase with a strong (200) texture. As such, the methodology presented herein represents a modified IME technique for the growth of high quality, epitaxial $CoSi_2$ films for applications in emerging microelectronics device technologies.
© 2000 The Electrochemical Society. S0013-465 1(00)09-080-7. All rights reserved.

Manuscript received September 25, 2000.

Self-aligned silicide (salicide) processing is an essential component of modern microelectronics technology. In this respect, titanium silicide ($TiSi_2$) is considered as the most widely used silicide for salicide functions in logic devices.[1] Alternatively, tungsten silicide ($WSi_2$) is typically used for gate applications in dynamic random access memory products.[2] However, as device dimensions scale down, increasingly more stringent requirements are being placed on the properties and performance of silicides, leading to the need for new materials and process technologies.[1] Cobalt silicide ($CoSi_2$) meets these requirements, such as low resistivity, low Si consumption, and high thermal and chemical stability.[3] Additionally, $CoSi_2$ provides the added advantage that its properties are independent of feature size and type of Si dopant.[4,5] Furthermore, relatively simple modifications in the process flow can allow the formation of epitaxial $CoSi_2$. The latter is highly desirable given the sharpness of the epitaxial $CoSi_2$/Si interface, thus enabling the formation of silicided shallow junctions with low contact resistance and low leakage characteristies.[6–8] Furthermore, agglomeration is dramatically reduced in the absence of grain boundaries resulting in superior thermal stability.[9–11]

The epitaxial growth of $CoSi_2$ on Si(100) should be enabled by the close lattice match between the $CoSi_2$ and Si crystal matrices which exhibit only ~1.2% lattice mismatch.[12] Unfortunately, the achievement of $CoSi_2$ epitaxy on Si(100) is not possible in the two-stage approach typically employed to grow $CoSi_2$ on Si. The latter involves, in first stage, the deposition of pure Co on Si, typically by physical vapor deposition (PVD) means. This step is followed, in a second stage, by a thermally driven solid state reaction with the Si substrate to grown $CoSi_2$.[12,13] In this case, an unrestricted supply of Co is available to the reaction process, with the rate limiting step being the formation of intermediate phases, primarily $Co_2So$ and CoSi, as a prelude to the growth of the $CoSi_2$ phase.[13] These phases are not epitaxially matched to Si, leading ultimately to the growth of polycrystalline $CoSi_2$.[13]

Clearly, the realization of epitaxy requires the elimination of the intermediate phases discussed above. This condition is achievable when the supply rate of Co to the silicidation reaction is sufficiently slow to allow the formation of the disilicide and the occurrence of epitaxial alignment at the same time.[13] One successful strategy to achieve this goal involves the insertion of an interfacial layer between Co and Si, a process commonly known as interlayer mediated epitaxy (IME). This method was first demonstrated with a titanium interlayer, which was referred to as titanium interlayer mediated epitaxy (TIME).[6,10,14–17] The typical TIME processing flow involves the *in situ,* sequential deposition of titanium then Co. Subsequent annealing causes the Co and titanium to first intermix around 300°C. Intermixing is followed by epitaxial growth of $CoSi_2$ at higher annealing temperature, with the titanium being driven to the surface of the resulting $CoSi_2$ phase.[3,6,10,14-17]

In the TIME process, titanium acts both as an oxygen getterer, by removing interfacial native oxide and reaction barrier, by preventing the formation of the intermediate $Co_2Si$ and CoSi phases. Both roles were believed to be equally crucial in the achievement of epitaxy.[3,6,10] However, a number of authors have recently suggested that although oxygen gettering is important, the role of titanium as reaction barrier is actually the key to $CoSi_2$ epitaxy.[8,18,19] For example, Selinder *et al.* showed that the presence of parts per million oxygen in the annealing gas was critical to $CoSi_2$ epitaxy. This behavior was attributed to the formation of a stable Co-Ti-O (spinel) membrane phase at the metal/Si interface.[19] The absence of oxygen led to the growth of the intermediate CoSi phase, which was followed by the formation of polycrystalline CoSi2.

Similarly, Tune reported the development of an oxide mediated epitaxy (OME) technique for epitaxial $CoSi_2$ formation.[11] The OME method involves the growth of a 0.5 to 1.5 nm thick, nonstoichiometric, $SiO_x$ ($x < 2$) interfacial layer by submerging the Si substrate in either a boiling $HCl:H_20_2:H_2O$ = 3:1:1 solution for 5 min. or a hot (90°C) $NH_4OH:H_20_2:H_2O$ = 1:1:4 solution for 20 min. In both cases, high quality epitaxial $CoSi_2$ was formed after annealing of a subsequently deposited Co layer, 1 to 3 nm thick, at 500-700°C. Tung argued that the thin $SiO_x$ layer acts as a diffusion barrier which delays the Co-Si reaction until the annealing temperature exceeds 500°C, thus inhibiting the formation of the intermediate $Co_2Si$ and CoSi phases. Interestingly, Tung observed that a thicker (20 Å) stoichiometrlc $SiO_2$ interfacial layer was detrimental to $CoSi_2$ epitaxy, with the resulting $CoSi_2$ layer being nonuniform and exhibiting poor epi-taxial quality.[11] Other workers also reported the observation of epitaxial $CoSi_2$ when germanium[20] or tantalum[21] are employed as interfacial barrier between Co and Si. Unlike traditional methods for epitaxial $CoSi_2$ growth, such as molecular beam epitaxy (MBE), the IME process is attractive because of its compatibility with standard complementary metal oxide semiconductor (CMOS) device fabrication flow. However, the introduction of a reaction barrier interlayer implies added process complexity because of the additional deposition and etching process steps required. Even though this is justified because of the significantly improved performance,[3,6,7] it is still highly desirable to identify a modified IME technique for the *in situ* formation of the interfacial and co layers as one unified growth process.

* Electrochemical Society Active Member
[d] Present Address: Genus, Inc., Sunnyvale, California 94089
[e] Present Address: Motorola APRDL, Austin, Texas 78721
[Z] E-mail: akaloyeros@uamail.albany.edu

*Journal of The Electrochemical Society,* **148** (1) C21-C27 (2001)
S0013-4651/2001/148(1)/C21/7/$7.00 © The Electrochemical Society, Inc.

Various cobalt source precursors have already been investigated for the chemical vapor deposition (CVD) of Co for magneto-optics applications,[22,23] magnetic Co-containing alloys,[24,25] *in situ* doping with Co,[26,27] and formation of epitaxial $CoSi_2$ for microelectronics device applications.[27-29] Among all potential sources, considerable attention was dedicated to the source precursor dicobalt octacarbonyl, $Co_2(CO)_8$. A serious drawback for its usage is the existence of undesirable, yet thermodynamically favorable, polymerization and hydrogenation reactions that compete with the formation of pure Co.[30] It is also known to be unstable during storage, even under vacuum or inert atmosphere.[31]

Instead, prior work by the present investigators has identified cobalt tricarbonyl nitrosyl, $Co(CO)_3NO$, as a worthy manufacturing source for CVD Co.[32] Its advantages include high vapor pressure (26 Torr at 0°C and 100 Torr at 25°C), availability in liquid form, and relatively good thermal stability during transport and handling. In addition, the existence of Co in zero oxidation state makes this precursor amenable to the clean breakage of metal-ligand bonds at low temperatures, leading to the deposition of pure Co.[32,33] In this report, results are presented from the successful application of this CVD Co process, in combination with a sacrificial titanium/titanium nitride (Ti/TiN) layer, for the growth of high quality, epitaxial $CoSi_2$ films for applications in emerging CMOS device technologies.

## Experimental

Cobalt films with thickness of 300 + 30 Å were deposited using thermal CVD from $Co(CO)_3NO$ as source precursor. Specific process details were reported elsewhere.[20] Deposition was performed in a standard custom designed, stainless steel alpha-type CVD reactor using Si(100) substrates. The Si(100) substrates were subjected to a predeposition, ex situ organic chemical clean consisting of an acetone and methanol rinse. The native oxide was subsequently etched in a 10% hydrofluoric acid solution followed by a deionized (DI) water rinse. Finally, the samples were dried in a high-purity argon atmosphere. Additional substrates used were nonpatterned silicon dioxide ($SiO_2$) and silicon nitride ($Si_3N_4$) on Si. The $SiO_2$ and $Si_3N_4$ layers had a thickness of, respectively, 250 and 80 nm. Both substrates were exposed to the same *ex situ*, redeposition, organic cleaning described above. These samples served as control samples during our subsequent annealing studies. The purpose was to ensure that the thermal treatment steps did not result in undesirable interactions between Co and the typical spacer materials used in actual device structures.

CVD Co films were deposited using the optimized process window displayed in Table I. The resulting films were divided into two splits. These splits were subsequently processed and annealed as described below. All annealing studies were performed in an AG Associates Heatpulse model 610 single wafer rapid thermal processor (RTP). In a typical annealing experiment, the sample was placed on a 5 in. carrier sensor wafer equipped with a K-type thermocouple. The thermocouple was used to provide real-time measurements of sample temperature during actual annealing. The oven was then purged with ultrahigh purity nitrogen (99.999%) for 10 min prior to each annealing step. All anneals were carried out in the same nitrogen ($N_2$) atmosphere. The temperature ramp rate was approximately 40°C/s. At the end of the annealing step, the heating lamps were turned off, and the sample was exposed to a cooling rate of 70 to 120°C/min, depending on the annealing temperature. Cooling was carried out in the ultrahigh purity $N_2$ atmosphere.

The first split (CVD split I) of CVD Co/Si was left uncapped and was annealed without any additional processing steps. Alternatively, CVD split II was capped with an overlayer consisting of 12 nm thick TiN on 10 nm thick titanium. The Co films were not subjected to any cleaning prior to the capping layer deposition in order to avoid any chemical changes in the Co surface.

The Ti/TiN capping layers were deposited *in situ,* using collimated dc sputter deposition on a commercial Varian MB2-830 sputtering cluster tool. Base pressure prior to deposition was in the $10^{-9}$ Torr range. Titanium was deposited using a titanium target. Sputtering was performed at room temperature, 2 mTorr process pressure, 40 standard cubic centimeters per minute (sccm) argon sputtering gas, and 100 mm target to substrate. TiN deposition was carried out with the same titanium target, using 65 sccm $N_2$ reactant gas, 40 sccm argon sputtering gas, a process pressure of 4 mTorr, and substrate to target spacing of 116 mm.

All splits were annealed at temperatures of 500, 550, 600, 650, 700, and 725°C. For each temperature, annealing was carried out for 30, 60, and 90 s. For the uncapped Co samples, unreacted Co metal from the annealed samples was removed by a 15 min etch in 10% nitric acid solution in deionized water. Alternatively, for the capped Co samples, the titanium and TiN capping layers were selectively etched in a solution of 3 $NH_4OH$: 1 $H_2O_2$:2 $H_2O$. This was followed by the Co etch recipe described above.

**Table I. Typical process parameters for thermal CVD Co from $Co(CO)_3NO$.**

| Parameter | Value |
|---|---|
| Substrate temperature | 390°C |
| Precursor flow rate | 0.5 sccm |
| Hydrogen reactant flow rate | 750 sccm |
| Process working pressure | 1.5 Torr |

Sputter-deposited, 30 ± 3 nm thick, Co films were annealed under the same experimental conditions used for the CVD Co and used as control samples in our silicidation studies. As in the case of the CVD Co samples, 2 splits of PVD Co were prepared. PVD split I was processed uncapped. PVD split II was capped with 12 nm thick TiN on 10 nm thick titanium.

## Analytical Techniques

The electrical, compositional, and structural properties of all samples were thoroughly analyzed using Rutherford backscattering spectrometry (RBS), four-point resistivity probe, X-ray diffraction (XRD), nuclear reaction analysis (NRA) for hydrogen profiling, and X-ray photoelectron spectroscopy (XPS), high-resolution transmission electron microscopy (HRTEM), and scanning electron microscopy (SEM). Resulting key CVD Co as-deposited film properties are presented in Table II.

**Table II. Summary of CVD Co key film properties.**

| Property (measurement technique) | Value |
|---|---|
| Oxygen, carbons nitrogen (XPS) | All below 1 atom % (detection limits of XPS) |
| Thickness (RBS and SEM) | 30 ± 3nm |
| Resistivity (four-point probe) | 15 ± 1.5 μΩ cm |
| Structure (XRD) | hcp Co |
| RMS surface roughness (AFM) | ~3.6 nm |
| Average surface grain size (AFM) | ~70 nm |

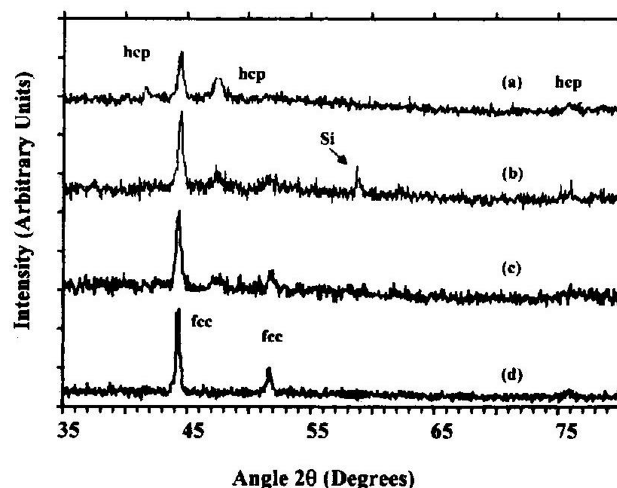


**Figure 1.** XRD patterns collected at low angle incidence for uncapped CVD Co films: (a) as-deposited, (b) annealed at 500°C for 30 s, (c) annealed at 600°C for 30 s, and (d) annealed at 700°C for 30 s. No silicidation is detected. Instead, a transformation from hcp Co to fcc Co is observed upon annealing.

*Journal of The Electrochemical Society,* **148** (1) C21-C27 (2001)
S0013-4651/2001/148(1)/C21/7/$7.00 © The Electrochemical Society, Inc.

RBS was employed to determine film thickness and composition. For this purpose, RBS data was compiled using a 2 MeV $He^+$ beam on a 4.5 MeV Dynamitron model P.E.E. 3.0 linear accelerator. Film thickness measurements were standardized using SEM on a Zeiss DSM 940 microscope, with a 20 keV primary electron beam. Four-point resistivity probe measurements were performed to determine sheet resistance. The film resistivity was then calculated using the thickness values measured with RBS and SEM. Nuclear reaction analysis for hydrogen profiling was performed on the same linear accelerator using the $15N(p, \alpha\gamma)^{12}C$ nuclear resonance reaction.

XRD analyses were done on a Scintag XDS 2000 X-ray diffractometer, equipped with a Cu Ka X-ray source and a horizontal wide angle four axis goniometer with stepping motors, which allowed in-dependent or coupled 0-2θ axes motion. XRD spectra for CVD Co were collected in both normal (Bragg-Bretano) and 5° low angle incidence geometry, and compared to the reference patterns in the Joint Committee for Powder Diffraction standards (JCPDS) Powder Diffraction File (PDF). Alternatively, XRD spectra for $CoSi_2$ films were collected only in normal geometry.

XPS was used to confirm our RBS findings in terms of film composition, as well as to determine elemental chemical states. XPS analyses were performed on a Perkin-Elmer PHI 5500 multitechnique system with spherical capacitor analyzer. The gold $f_{7/2}$ line was used as a reference and the analyzer calibrated accordingly. The primary X-ray beam was generated with a monochromatic Al Kα X-ray source at operating power of 300 W and 15 keV applied to the anode. The use of Al Kα primary X-rays allowed the elimination of undesirable interference between the co LMM and O 1s peaks. Depth profiles were acquired after a 30 s or 1 min long sputter clean cycle. The oxygen 1s peak window (544 to 526 eV) was scanned first after each sputtering cycle in order to avoid any potential oxygen loss in the vacuum

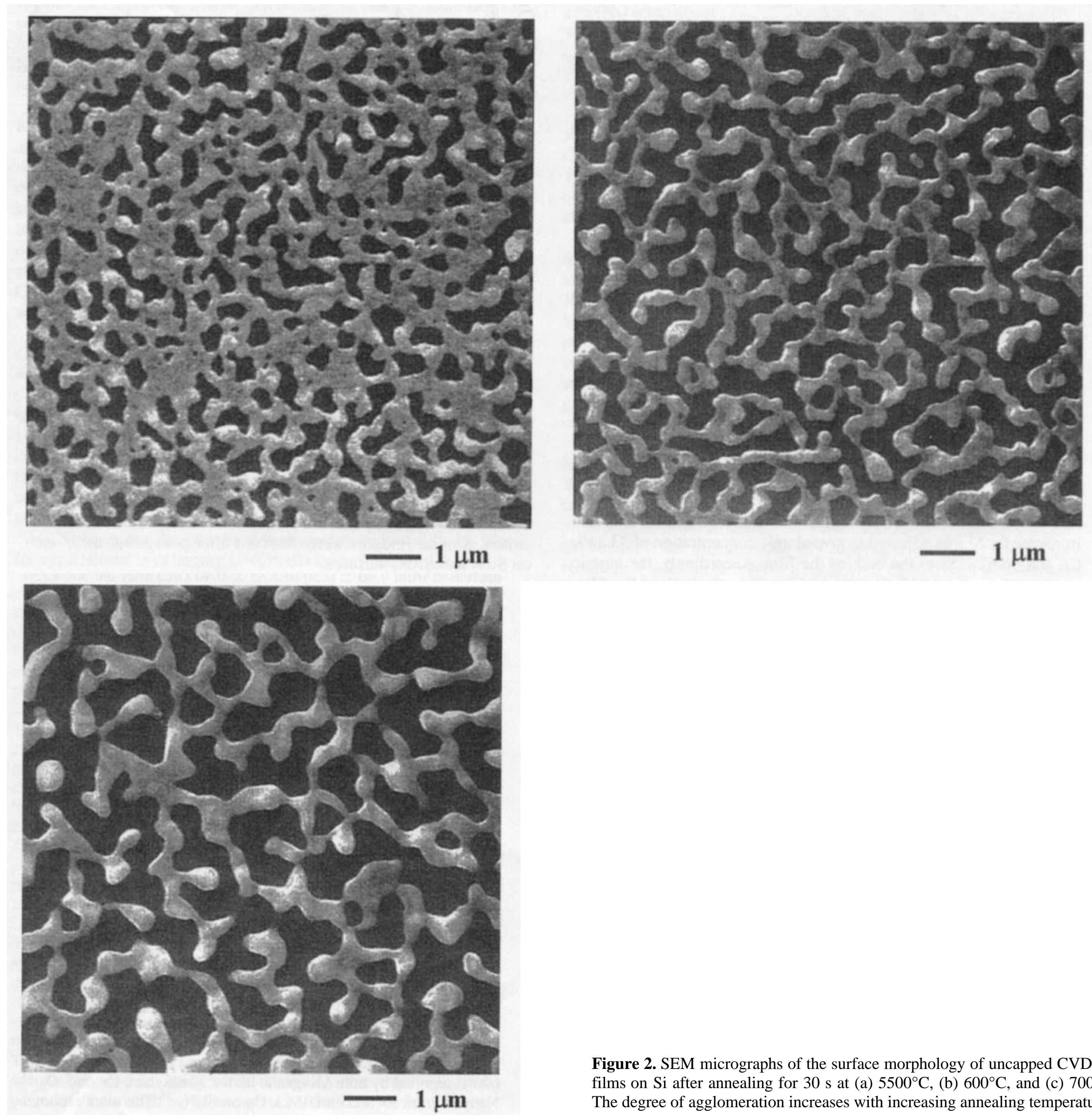


**Figure 2.** SEM micrographs of the surface morphology of uncapped CVD Co films on Si after annealing for 30 s at (a) 5500°C, (b) 600°C, and (c) 700°C. The degree of agglomeration increases with increasing annealing temperature.

*Journal of The Electrochemical Society,* **148** (1) C21-C27 (2001)
S0013-4651/2001/148(1)/C21/7/$7.00 © The Electrochemical Society, Inc.

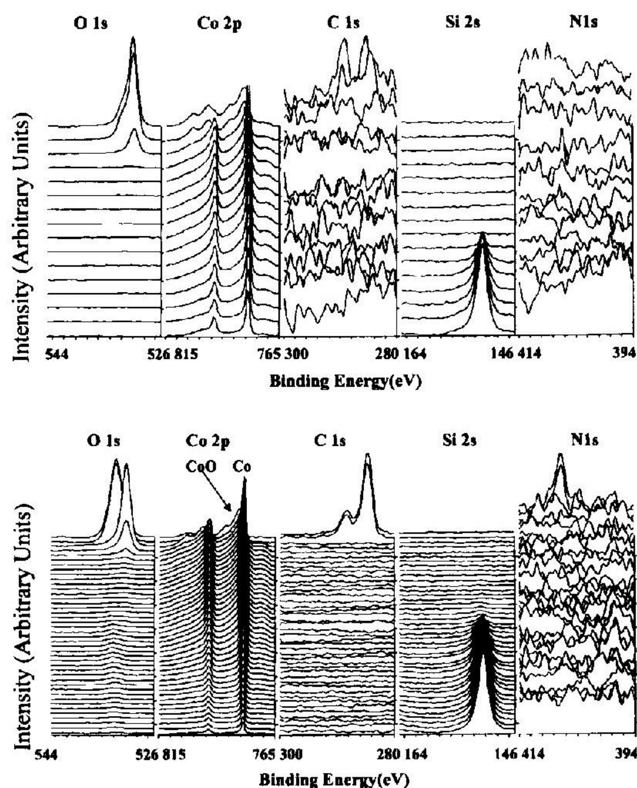


**Figure 3.** XPS depth profile of key elemental core peaks for (a, top) PVD-deposited and (b, bottom) CVD-deposited uncapped Co samples.

system. The Si 2s (150.5 eV) peak was monitored in order to avoid any interference between the Co 3s (101 eV) and Si 2p (99.3 eV) peaks. The photoelectron peak heights were converted to atomic concentration using elemental sensitivity factors. A reference 1000 Å thick $CoSi_2$ sample was analyzed and the sensitivity factor for Si was adjusted to give atomic concentration of 33.33% Co and 66.67% Si in the bulk of the film. Accordingly, the atomic concentration values were recalculated for all samples analyzed.

HRTEM was performed on a JOEL 2010F field emission electron microscope operating at 200 kV. Imaging was performed with the sample tilted so that the Si<110> zone axis was perpendicular to the incident beam. Cross-sectional TEM specimens were prepared by standard sample preparation procedures, including mechanical sample polishing, dimpling, and argon ion milling. TEM analysis was performed on the thinnest region (<50 nm) adjacent to the center hole in the sample.

## Results and Discussion

*Silicidation studies of uncapped Co samples.* — In the case of the uncapped PVD Co/Si samples (PVD split I), XRD studies indicated the formation of the CoSi phase after the 500°C, 30 s anneal, with the corresponding XRD pattern being in excellent agreement with the JCPDS PDF no. 08-0362. Alternatively, XRD showed that the 600°C, 30 s anneal was sufficient for the complete transformation of Co into a randomly oriented polycrystalline $CoSi_2$ phase, with the corresponding XRD pattern yielding diffraction peaks that are in excellent agreement with the JCPDS PDF no. 38-1449. The XRD findings were supported by our RBS and sheet resistance measurements, with the 100 nm thick $CoSi_2$ phase exhibiting a sheet resistance and resistivity values of, respectively, 2.0 ± 0.3 Ω/□ and 19 ± 2 μΩ cm. As expected, epitaxial $CoSi_2$ was not formed across the entire thermal treatment window investigated.

In the case of uncapped CVD Co samples (CVD split I), XRD analyses showed that the as-deposited hexagonal close packed (hcp) Co phase was transformed into the face centered cubic (fcc) Co phase, as illustrated in Fig. 1. Interestingly, no XRD peaks corresponding to any of the cobalt silicide or cobalt oxide phases were detected in samples annealed in the entire rapid thermal anneal (RTA) process window investigated.

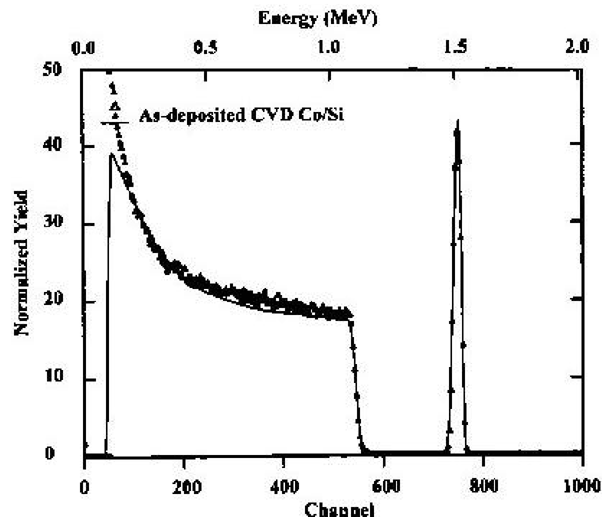


**Figure 4.** Typical RBS spectrum and associated simulation curve for a 30 nm thick CVD Co film.

Selective chemical etching studies of the annealed co samples confirmed XRD findings with respect to the absence of any cobalt silicide phase. In this respect, the 15 min etch in 10% nitric acid solution in DI water was successful at completely removing the entire film from the Si substrates, a behavior that supports the suggestion that neither CoSi nor $CoSi_2$ were formed. RBS analyses of postwet etched samples showed that within the detection limits of RBS, no Co or cobalt silicide phases were detected on the Si substrates. Similar findings were observed after postanneal metal etch on $SiO_2$ and $Si_3N_4$ surfaces.

Sheet resistance measurements showed that sheet resistance decreased from 4.40 ± 0.50 to 3.85 ± 0.40 Ω/□ after the 500°C/30 s anneal, which corresponds to a decrease in resistivity from 15.0 ± 1.5 to 12.0 ± 1.2 μΩ cm. With further increase in annealing temperature, the sheet resistance was found to increase rapidly with, for example, the sample annealed at 700°C/30 s exhibiting a sheet resistance above 1 k Ω/□.

Prior to the wet etch step, all annealed samples were also analyzed by SEM in order to examine the evolution of film surface morphology. SEM analyses showed Co film agglomeration for all samples annealed at temperatures above 500°C. As an example, the SEM images of Co films annealed at 500, 600, and 700°C for 30 s are shown in Fig. 2. It is clearly seen that the degree of agglomeration increased with high annealing temperature, and the Co film became practically discontinuous after the 600°C/30 s anneal. The SEM results correlated well with the findings from the sheet resistance

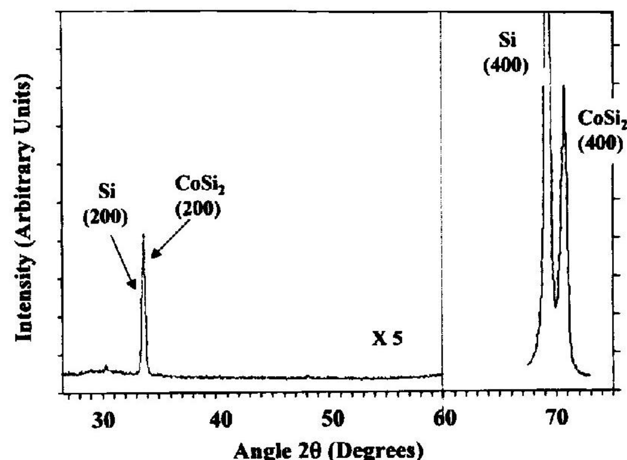


**Figure 5.** Normal incidence XRD spectrum for a Ti/TiN capped CVD Co film after annealing at 725°C for 30 s, and selective etch of the Ti/TiN and unreacted Co layers. XRD data indicates the formation of an epitaxial $CoSi_2$ phase.

S0013-4651/2001/148(1)/C21/7/$7.00 © The Electrochemical Society, Inc.

measurements. In particular, the initial decrease in the sheet resistance after

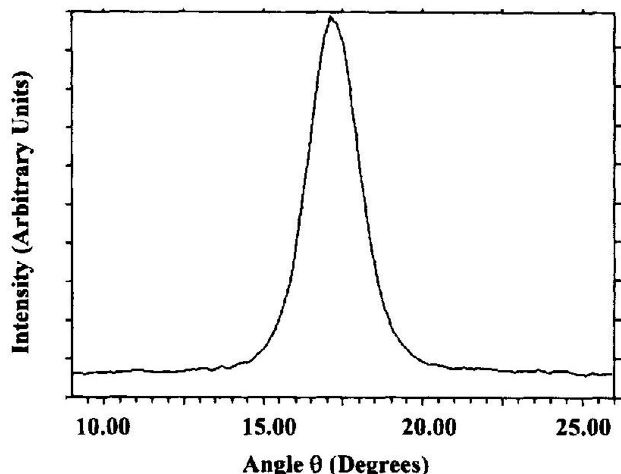


**Figure 6.** XRD rocking curve (theta scan) measurement for epitaxial $CoSi_2$ (400) reflection. The corresponding fwhm wa found to be 1.11°, as compared to fwhm of 0.7° for the (400) diffraction peak from the single crystal Si substrate.

the 500°C/30 s anneal was attributed to Co grain coalescence and growth. The more severe Co film agglomeration occurring at higher annealing temperatures, leading to the formation of separate Co islands, resulted in the observed rapid increase of sheet resistance values.

Interestingly, similar results were previously reported for annealed Co films on $SiO_2$ and $Si_3N_4$.[34-37] The agglomeration was attributed to a lowering of the overall energy of the system through reduction of the Co/dielectric interfacial area.[34-37] However, an earlier onset temperature of agglomeration was observed here than the 600°C reported by both Morgan *et al.* for 30 nm thick Co on $SiO_2$,[34] Nguyen *et al.* for 12.5 nm thick Co on $Si_3N_4$.[36] The work reported herein also showed that under the same RTA conditions, Co films on $SiO_2$ and $Si_3N_4$ exhibited a lower degree of Co agglomeration as compared to their counterpart on Si.

In order to elucidate the mechanisms that drive the observed agglomeration phenomenon, the composition of the CVD split I and PVD split I was subjected to thorough investigation by XPS and RBS. Accordingly, typical high resolution XPS core peak spectra as a function of film depth are displayed in Fig. 3a and b for, respectively, the PVD and CVD samples. In both cases, no oxygen, carbon, or nitrogen contaminants were detected in the bulk of the films within the detection limits of XPS (<1 atom %). However, a 2.7 atom % oxygen contamination was detected at the Co-Si interface for the CVD Co films, as indicated in Fig. 3b. This contamination could not be attributed to native oxygen on the Si substrate surface, given that all Si samples were subjected to the same wet chemical treatment prior to CVD and PVD processing, and that no oxygen was detected at the Co-Si interface for the PVD Co films.

In this respect, the XPS O 1s peak position for interfacial oxygen was 532 eV. This value is consistent with the presence of a Si-O phase or a Co-Si-O phase, which exhibit O 1s peaks at, respectively, 532.5 and 531.6 eV.[38] It could not be attributed to a cobalt oxide phase, given that the O 1s peak locations are 530.1 and 529.6-530.2 eV for, respectively, CoO and $Co_3O_4$. RBS data confirmed our XPS findings in terms of film bulk composition, and indicated the absence of any heavy element contaminants in both sets of films. This is illustrated in Fig. 4, which displays a typical RBS spectrum and associated simulation curve for a 30 nm thick CVD Co film. NRA studies indicated the absence of hydrogen in the Co film, as well as at the Co-Si interface.

*Silicidation studies of Ti/TiN capped Co samples.* The studies described above were repeated for PVD split II and CVD split II, which are PVD and CVD Co samples capped with a Ti/TiN bilayer (as explained previously in the Experimental section). The purpose was to suppress agglomeration and lower the energy barrier to cobalt silicide formation. The Ti layer was used partially to getter any oxygen from the surface of the air-exposed Co film, while a TiN cap was employed in order to prevent oxidation of the Ti layer upon air exposure.

In the case of the Ti/TiN capped PVD samples (PVD split II), XRD measurements were performed after selective etching of the Ti/TiN and unreacted Co layers. The results indicated for formation of a polycrystalline $CoSi_2$ phase with a strong (200) texture, in agreement with prior results for Ti capped PVD Co films.[39] The structure of this $CoSi_2$ phase was independent of the temperature and duration of the annealing experiments. Corresponding resistivity was 21.0 + 4.0 μΩ cm. As in the case of uncapped PVD Co, no epitaxial $CoSi_2$ phase was formed across the entire thermal treatment window investigated.

In the case of CVD split II, XRD measurements were also performed after selective etching of the Ti/TiN and unreacted Co layers. For illustration purposes, Fig. 5 presents the typical normal incidence XRD spectrum for the sample annealed at 725°C for 30 s, after selective etch of the Ti/TiN and unreacted Co layers. As can be seen, high intensity peaks associated with the $CoSi_2$ (200) and (400) reflections were observed in this case, along with the Si(200) and Si(400) contributions from the underlying substrate. As such, the normal incidence XRD data indicated the existence of an epitaxial $CoSi_2$ phase. The degree of epitaxy was evaluated by performing an XRD rocking curve (theta scan) measurement for the $CoSi_2$ (400) reflection, as displayed in Fig. 6. The corresponding full width at half maximum (fwhm) was found to be

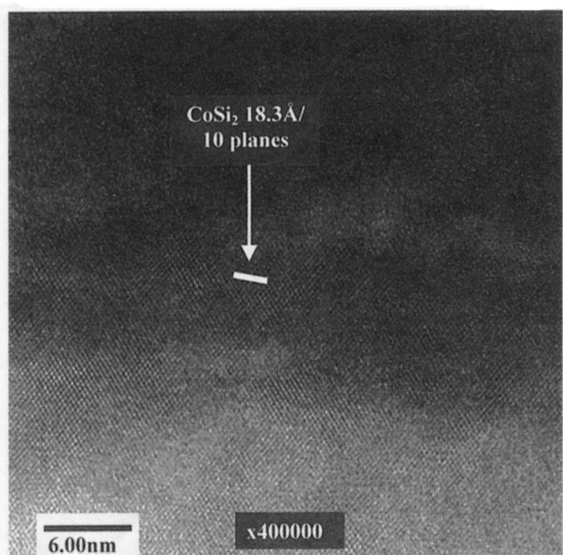


**Figure 7.** HRTEM bright field image, collected along the Si<100> zone axis, of an epitaxial $CoSi_2$ film annealed at 725°C for 30 s.

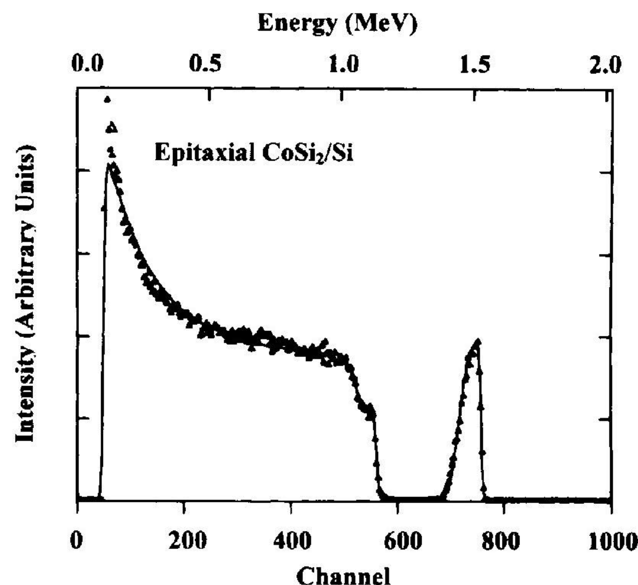


**Figure 8.** Typical RBS spectrum and associated simulation curve for epitaxial $CoSi_2$ on Si, after selective etch of the Ti/TiN and unreacted Co layers.

1.11%, as compared to a fwhm of 0.7° for the (400) diffraction peak from the single crystal Si substrate.

HRTEM bright field imaging studies confirmed the XRD findings regarding the formation of epitaxial $CoSi_2$ films. The corresponding HRTEM micrograph, collected along the Si<100> zone axis, of an epitaxial $CoSi_2$ film annealed at 725°C for 30 s is shown in Fig. 7. Compete coherence was observed between the $CoSi_2$ layer and the underlying Si substrate. RBS analyses showed the formation of 1000 Å thick epitaxial $CoSi_2$ layer, as illustrated in Fig. 8. A comparison of the integrated intensity for the RBS co peak for the as-deposited sample *vs.* its counterpart after annealing and selective metal etching indicated that ~90% of the CVD Co film was consumed in the silicide reaction.

An XPS depth profile of the postannealed samples showed constant Co to Si ratio throughout the bulk of the silicide. Titanium, carbon, and nitrogen were below the detection limits of XPS. The levels of oxygen in the bulk of the $CoSi_2$ film and at the silicide/Si interface were, respectively, slightly below ~ 1.5 and ~3.0 atom %. Film resistivity was ~23.10 μΩ cm. This value is slightly higher than that observed for the PVD films, and is attributed to the presence of residual oxygen in the $CoSi_2$ phase, which is believed to have resulted from air exposure of the Co film prior to the Ti/TiN deposition step. This observation is consistent with the work of Tung, who reported slight degradation in the epitaxial quality of $CoSi_2$ films when the Co layer was exposed to air.[11]

*Discussion.* — Within the CVD co process window investigated, the data presented above seem to indicate that an ultrathin Si-O or Co-Si-O layer was inherently formed at the Co-Si interface during the CVD growth process. This assessment is supported by the observation of oxygen at the Co-Si interface, with the corresponding XPS O 1s peak shape and location being consistent with those from a Si-O or Co-Si-O layer. The presence of interfacial oxygen could not be attributed to native oxide on the Si substrate surface, given that all Si samples were subjected to the same wet chemical treatment prior to CVD and PVD processing, and no oxygen was detected at the Co-Si interface for the PVD Co films. The thickness of this interlayer was below the sensitivity limits of RBS and SEM (≤ 100 Å). However, based on XPS sputter times and associated ionic yields, it was estimated to be ~50 Å.

In this respect, the existence of the interfacial oxide layer is in agreement with prior work in the literature by Roustan et *al.*[40] on the room temperature adsorption and reaction of $Co(CO)_3NO$ on catalytic surfaces, and with our previous work on the development and optimization of a thermal Co CVD process.[32] In particular, Roustan *et al.* examined the room temperature adsorption and reaction path-ways of Co(CO)3NO on a catalytic surface, namely, activated alu-mina. By applying time-resolved Fourier transform infrared spec-troscopy (FTIR) and mass spectrometry, Roustan *et al.* were able to observe the adsorption of CoNOCO radicals to the alumina surface. They also noted the formation of isocyanates (NCO) from the NO and CO groups, with the co atom being the most likely candidate to act as an acceptor of the extra oxygen atom. The present investiga-tors observed similar results in their prior work,[32] with either Co or Si being suggested as the probable recipients of the extra oxygen, leading to the formation of an interfacial Si-O or Co-Si-O layer. The thickness of the interfacial oxide layer is believed to be inversely proportional to the CVD processing temperature.

The Si-O or Co-Si-O interlayer appears to inhibit silicidation in the case of uncapped CVD Co samples (CVD split I). This conclusion is supported by the failure to initiate silicidation for uncapped CVD Co samples, regardless of the temperature and duration of the annealing step. Alternatively, formation of the Co Si phase was achieved for PVD Co samples of identical thickness after a 500°C, 30 s anneal under identical conditions to those used for the CVD samples. Additionally, a 600°C, 30 s anneal was sufficient for the complete transformation of PVD Co into a randomly oriented polycrystalline $CoSi_2$ phase.

Instead, the presence of the interfacial layer in the case of CVD split I appears to have caused agglomeration of CVD Co during the annealing studies, with the degree of agglomeration being proportional to the annealing temperature. Similar results were previously reported for annealed Co films on $SiO_2$ and $Si_3N_4$.[34–47] This agglomeration is attributed to a lowering of the overall energy of the system through reduction of the Co/substrate interfacial area.

Alternatively, for Ti/TiN capped CVD Co samples (CVD split II), the interfacial layer appears to play a role similar to that observed for similar layers in IME. This conclusion is supported by the observation of epitaxial $CoSi_2$ for capped CVD Co samples after a 725°C, 30 s anneal, on contrast, similarly capped PVD Co samples annealed under identical processing conditions exhibited a polycrystalline $CoSi_2$ phase with a strong (200) texture, in agreement with prior results for Ti capped PVD Co films.[39]

As in the case of IME, the interfacial layer is believed to have acted to limit the Co supply rate to the silicidation reaction, thus allowing the formation of the disilicide and the occurrence of epitaxial alignment at the same time.[13] In this respect, our findings are in agreement with the work of Selinder *et al.,* who showed that the presence of parts per million oxygen in the annealing gas was critical to $CoSi_2$ epitaxy. This behavior was attributed to the formation of a stable Co-Ti-O (spines membrane phase at the metal/Si interface.[19] In that case, the absence of oxygen led to the growth of the intermediate CoSi phase, which was followed by the formation of polycrystalline $CoSi_2$.

Our results are also consistent with the findings of Tung, who reported the development of an OME technique for epitaxial $CoSi_2$ formation.[11] As discussed earlier, the OME method involved the growth of a 0.5 to 1.5 mm thick, nonstoichiometric, $SiO_x$ ($x < 2$) interfacial layer. In that case, high quality epitaxial $CoSi_2$ was formed after annealing of a subsequently deposited Co layer, 1 to 3 nm thick, at 500-700°C.

The intensity ratio of the XRD (400):(200) reflection peaks for epitaxial $CoSi_2$ was estimated to be ~10:1. Intensity ratios in the same range, namely, 7:1 to 14: 1, were reported by Zhang *et al.*[15] for epitaxial $CoSi_2$ grown by the TIME process. In this respect, Zhang *et al.* calculated a value of 31:1 for the XRD (400);(200) reflection peak ratio for their epitaxial $CoSi_2$ films, assuming a calcium fluoride ($CaF_2$) structure of infinite thickness. Alternatively, Zhang *et al.* obtained a value of 5:1 for the same peak ratio, under the assumption of a metastable diamond structure. By comparing these calculations with their experimentally observed reflection peak ratio, they argued that during the initial stages of growth, epitaxial $CoSi_2$ forms as a metastable diamond structure. It is thus suggested that the observation of a similar structure in our films might provide another indication of a TIME-like growth mode, according to the hypothesis of Zhang *et al.*[15] In this respect, the Ti/TiN capping layer acted to suppress Co agglomeration during the annealing step, and allowed Co diffusion uniformly through the interlayer into Si.

## Conclusions

Results were presented from the development of a new CVD-based approach for the formation of epitaxial $CoSi_2$. This CVD approach exploits the reaction kinetics associated with the adsorption and decomposition of $Co(CO)_3NO$ on Si surfaces to ensure the *in situ,* sequential growth of an ultrathin interfacial oxide layer followed by a Co thin film in a single low temperature (390°C) deposition step. It was observed that the interlayer, consisting of a Si-O or a Co-Si-O phase, prevented silicidation for uncapped CVD Co at all annealing times and temperatures investigated. Instead, Co agglomeration was observed, with the degree of agglomeration being directly proportional to the annealing temperature. The agglomeration was attributed to a reduction in the overall energy of the system through decrease of the Co/Substrate interfacial area. Alternatively, for Ti/TiN capped CVD Co samples, the interfacial layer appeared to play a role similar to that observed for similar layers in IME. This assessment is supported by the observation of epitaxial $CoSi_2$ for capped CVD Co samples after a 725°C, 30 s anneal. In contrast, similarly capped PVD Co samples annealed under identical processing conditions exhibited a polycrystalline $CoSi_2$ phase with a strong (200) texture. As such, the methodology presented herein represents a modified IME technique for the growth of high quality epitaxial $CoSi_2$ films for applications in emerging microelectronics device technologies.

## Acknowledgments

The work was supported by the New York State Center for Advanced Thin Film Technology (CAT), Gelest, Inc. and MKS Instruments, Inc. Their support is gratefully acknowledged.

*The University at Albany-State University of New York assisted in meeting the publication costs of this article.*

## References

1. B. El-Kareh, *Fundamentals of Semiconductor Processing Technologies,* Kluwer Academic Publishers, Norwell, MA (1995).
2. T. Kikkawa and I. Sakai, *Mater: Res. Soc. Symp. Proc.,* **402**, *199 (1996).*

3. M. J. Scherony, T. S. Sriram, C. England, A. Pelillo, W. C. Hams, S. J. Miller, S. A. Bill, T. Y. Yang, A. Wei, and D. A. Antoniadis, *Mater. Res. Soc. Symp. Symp. Proc.,* **404**, 209 (1996).
4. E. G. Colgan, J. P. Cambino, and Q. Z. Hong, *Mater: Sci. Eng.,* **R16**, 43 (1996).
5. K. Maex, *Mater: Sci. Eng.,* **R11**, 53 (1993).
6. M. Lawrence, A. Dass, D. B. Fraser, and C.-S. Wei, *Appl. Phys. Lett.,* **58**, 1308 (1991).
7. Q. F. Wang, A. Lauwers, F. Jonckx, M. de Potter, C.-C. Chen, and K. Maex, *Mater. Res. Soc. Symp. Proc.,* **402**, 221 (1996).
8. G. B. Kim, S. J. Kwak, H. K. Baik, and S. M. Lee, J. *Appl. Phys.*, **82**, 2323 (1997).
9. G. Bai and R. Stivers, *Mater. Res. Soc. Symp. Proc.,* **402**, 215 (1996).
10. S. L. Hsia, T. Y. Tan, P. Smith, and G. E. McGuire, J. *Appl. Phys.,* **70**, *7579 (*1991 ); S. L. Hsia, T. Y. Tan, P. Smith, and G. E. McGuire, J. *Appl. Phys.,* **72**, 1864 (1992).
11. R. T. Tung, *Appl. Phys. Lett.,* **68**, 3461 ( 1996).
12. M. A. Nicolet and S. S. Lau, in *VLSI Electronics: Microstructure Science, Vol. 6,* N. G. Einspruch and G. B. Larrabee, Editors, p. 330, Academic Press, New York (1983).
13. A. H. Reader, A. H. van Ommen, P. J. Weijs, R. A. M. Wolters, and D. J. Oostra, *Rep. Prog. Phys.,* **56**, 1397 ( 1992).
14. A. Vantomme, M.-A. Nicolet, G. Bai, and D. B. Fraser, *Appl. Phys. Lett.,* **62**, *243* (1992).
15. S.-L. Zhang, J. Cardenas, F. M. d'Heurle, B. G. Svensson, and C. S. Petersson, *Appl. Phys. Lett.,* **66**, *59* (1995).
16. G. B. Kim, H. K. Baik, and S. M. Lee, *Appl. Phys. Lett.,* **69**, 3498 (1996).
17. S. Hong, P. Wetzel, G. Gewinner, and C. Pirri, J. *Vac. Sci. Technol.* A, **14**, 3236 (1996).
18. R. Pretorius and J. W. Mayer, J. *Appl. Phys.,* **81**, 2448 (1997).
19. T. I. Selinder, D. J. Miller, and K. E. Gray, *Appl. Phase. Lett.,* **67**, 1597 (1995).
20. J. S. Byun, D.-H. Kim, W. S. Kim, and H. J. Kim, J. *Appl. Phys.,* **78**, 1725 (1995).
21. S. W.-K. Choi and R. J. Puddephatt, *Chem. Mater.,* **9**, 1191 (1997).
22. T. Maruyama and T. Nakai, *Appl. Phys. Lett.,* **59**, *1433 (* 1991).
23. D. K. Liu, U.S. Pat. 5,171,610 (Dec 1992).
24. R. S. Dickson, P. Yin, M. Ke, J. Johnson, and G. B. Deacon, *Polyhedron,* **15**, 2237 ( 1996).
25. K. L. Hess, S. W. Zehr, W. H. Cheng, J. Pooladdej, K. D. Buehring, and D. L. Wolf, *J. Cryst. Growth,* **93**, 576 (1988).
26. K. L. Hess and S. W. Zehr, U.S. Pat. 5,045,496 (1998).
27. M. E. Gross, K. Schnoes Kranz, D. Brasen, and H. Luftman, *J. Vac. Sci. Technol., B*, **6**, 1548 (1988).
28. H. S. Rhee and B. T. Ahn, *J. Electrochem. Soc.,* **146**, 2720 ( 1999).
29. G. A. West and K. W. Beeson, *Appl. Phys. Lett.,* **53**, 740 ( 1988).
30. J. P. Candlin, K. A. Taylor, and D. T. Thompson, *Reactions of Transition-Metal Complexes,* Elsevier Publishing Co., New York (1968).
31. C. J. Smart, S. K. Reynolds, C. L. Stanis, A. Patil, and J. T. Kirleis, *Maters Res. Soc. Symp. Proc*., **282**, 229 (1993).
32. A. R. Ivanova, G. Nuesca, X. Chen, C. Goldberg, B. Arkles, J. J. Sullivan, and A. E. Kaloyeros, J. *Electrochem. Soc.,* **146**, 2139 ( 1999).
33. J. A. Mattern and S. J. Gill, in *The Chemistry of the Coordination Compound., J. C.* Bailar, Jr., Editor, p. 509, Reinhold Publishing Co., New York (1956).
34. A. E. Morgan, E. K. Broadbend, M. Delfino, B. Coulman, and D. K. Sadana, J. *Electrochem. Soc.,* **134**, 925 (1987).
35. A. E. Morgan, K. N. Ritz, and E. K. Broadbend, A. S. Bhansali, J. *Appl. Phys.,* **67**, 6265 (1990).
36. H. L. Ho, T. Nguyen, J. C. Chang, B. Machesney, and P. Geiss, J. *Mater. Rev.,* **8**, 467 (1993).
37. T. Nguyen, H. L. Ho, D. E. Kotecki, and T. D. Nguyen, J. *Appl. Phys.,* **79**, 1124 (1996).
38. *Handbook of X-Ray Photoelectron Spectroscopy,* Perkin-Elmer Corporation, Physical Electronics Division (1979).
39. R. T. Tung and F. Schery, *Appl. Phys. Lett.,* **67**, *2164 (* 1995).
40. J. L. Roustan, Y. Lijour, and B. A. Morrow, *Inorg. Chem.,* **26**, 2509 (1987).